Supplement of Biogeosciences, 20, 4711–4736, 2023
https://doi.org/10.5194/bg-20-4711-2023-supplement

Biogeosciences Open Access EGU

Supplement of

Unique ocean circulation pathways reshape the Indian Ocean oxygen minimum zone with warming

Sam Ditkovsky et al.

Correspondence to: Sam Ditkovsky (samjd@princeton.edu) and Laure Resplandy (laurer@princeton.edu)

Name	<10 μmol/kg (AS)	<20 μmol/kg (AS)	<20 μmol/kg (BB)	<60 μmol/kg	<150 μmol/kg
WOA	0.2	1.8	0.6	8.3	20.9
GFDL-CM4	0.3	0.5	1.2	5.0	17.9
GFDL-ESM4	0.4	0.6	1.3	4.8	18.1
MIROC-ES2L	0.5	0.8	1.2	5.9	20.7
MPI-ESM1-2-HR	1.2	1.6	2.5	9.7	20.9
MPI-ESM1-2-LR	1.8	2.6	2.5	10.0	19.3
NorESM2-LM	1.6	2.2	2.6	9.4	21.3
NorESM2-MM	2.0	2.6	2.7	9.5	20.5
UKESM1-0-LL	0.3	0.6	0.9	4.4	17.4
ACCESS-ESM1-5	0.0	0.0	0.4	2.7	19.2
CanESM5	0.0	0.0	0.4	1.6	17.5
CanESM5-CanOE	0.0	0.0	0.9	4.1	20.8
CNRM-ESM2-1	0.0	0.5	1.4	8.7	22.6
IPSL-CM6A-LR	0.0	0.0	0.1	0.7	19.2
MRI-ESM2-0	0.0	0.0	1.4	3.5	18.8

Table S1. Thermocline OMZ volume, $\mathcal{V}^{1000\mathrm{m}}$, in units of $10^{15}\mathrm{m}^3$

Table S2. ESM data discarded from primary analysis, but presented in supplementary materials. Variables used: Dissolved oxygen concentration (o2), salinity (so), potential temperature (thetao), ideal age (agessc), export of organic carbon at 100 m (epc100), and mass transport (umo/vmo) where available. All data used is publicly available via ESGF.

ESM	Variables	Member ID
ACCESS-ESM1-5 (Ziehn et al., 2019a, b)	o2, thetao, so, agessc, epc100, umo/vmo	r1i1p1f1
CNRM-ESM2-1 (Seferian, 2018, 2019)	o2, thetao, so, epc100	r1i1p1f2
CanESM5 (Swart et al., 2019a, d)	o2, thetao, so, agessc, epc100, umo/vmo	r1i1p1f1
CanESM5-CanOE (Swart et al., 2019b, c)	o2, thetao, so, agessc, epc100	r1i1p2f1
IPSL-CM6A-LR (Boucher et al., 2018, 2019)	o2, thetao, so, epc100, umo/vmo	r2i1p1f1
MRI-ESM2-0 (Yukimoto et al., 2019a, b)	o2, thetao, so, epc100, umo/vmo	r1i2p1f1

References

Boucher, O., Denvil, S., Levavasseur, G., Cozic, A., Caubel, A., Foujols, M.-A., Meurdesoif, Y., Cadule, P., Devilliers, M., Ghattas, J., Lebas, N., Lurton, T., Mellul, L., Musat, I., Mignot, J., and Cheruy, F.: IPSL IPSL-CM6A-LR model output prepared for CMIP6 CMIP, https://doi.org/10.22033/ESGF/CMIP6.1534, 2018.

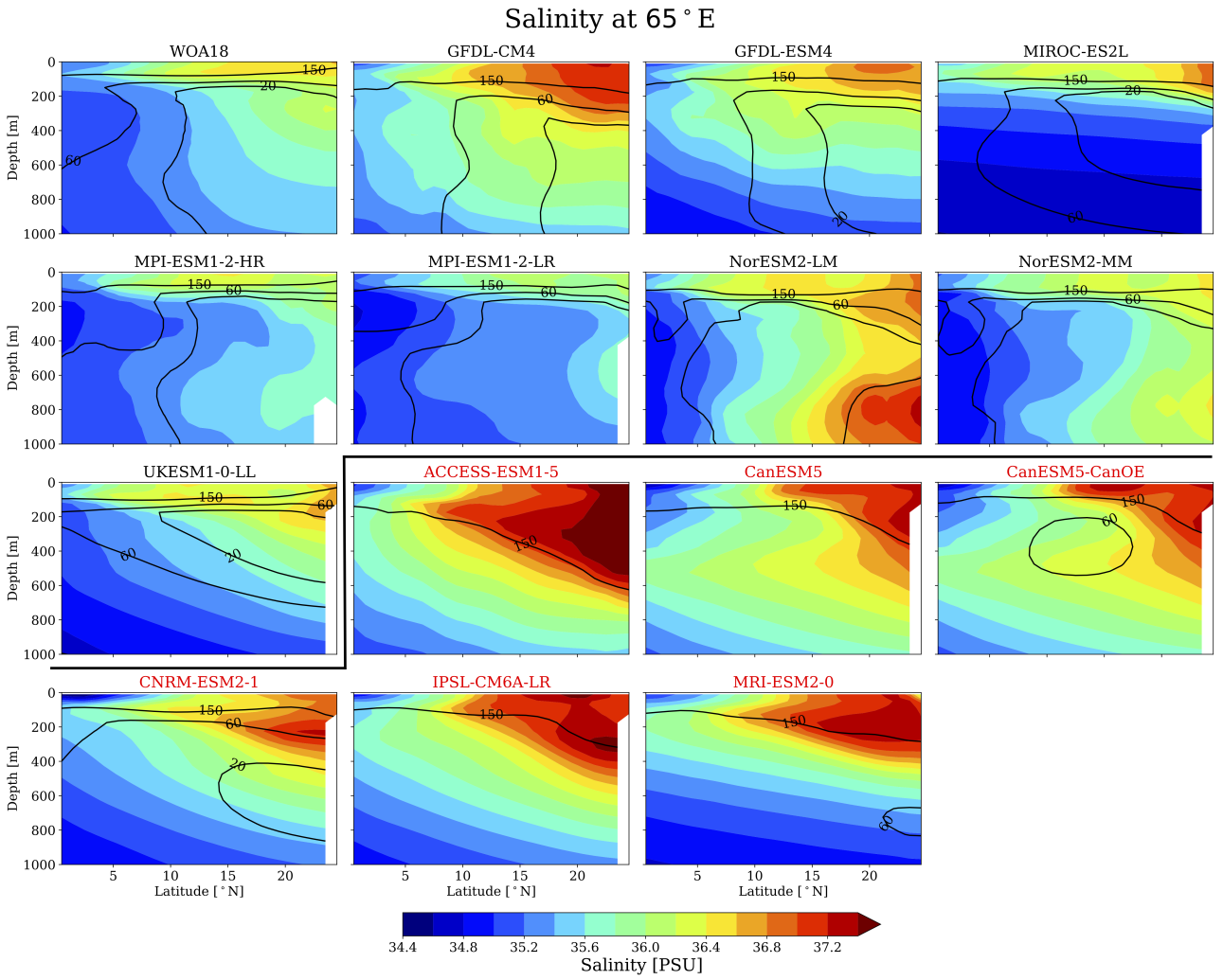

Figure S1. Sections of salinity along 65° E in the Arabian Sea for observed climatology (WOA18) and individual CMIP6 ESMs. Contours show 20, 60, and 150 μmol/kg oxygen extent. Models labeled in black are used in the ESM ensemble, while models labeled in red have been omitted

Boucher, O., Denvil, S., Levavasseur, G., Cozic, A., Caubel, A., Foujols, M.-A., Meurdesoif, Y., Cadule, P., Devilliers, M., Dupont, E., and Lurton, T.: IPSL IPSL-CM6A-LR model output prepared for CMIP6 ScenarioMIP, https://doi.org/10.22033/ESGF/CMIP6.1532, 2019.

Seferian, R.: CNRM-CERFACS CNRM-ESM2-1 model output prepared for CMIP6 CMIP, https://doi.org/10.22033/ESGF/CMIP6.1391, 2018.

Seferian, R.: CNRM-CERFACS CNRM-ESM2-1 model output prepared for CMIP6 ScenarioMIP, https://doi.org/10.22033/ESGF/CMIP6.1395, 2019.

Sofianos, S. S. and Johns, W. E.: Observations of the summer Red Sea circulation, Journal of Geophysical Research: Oceans, 112, 2007.

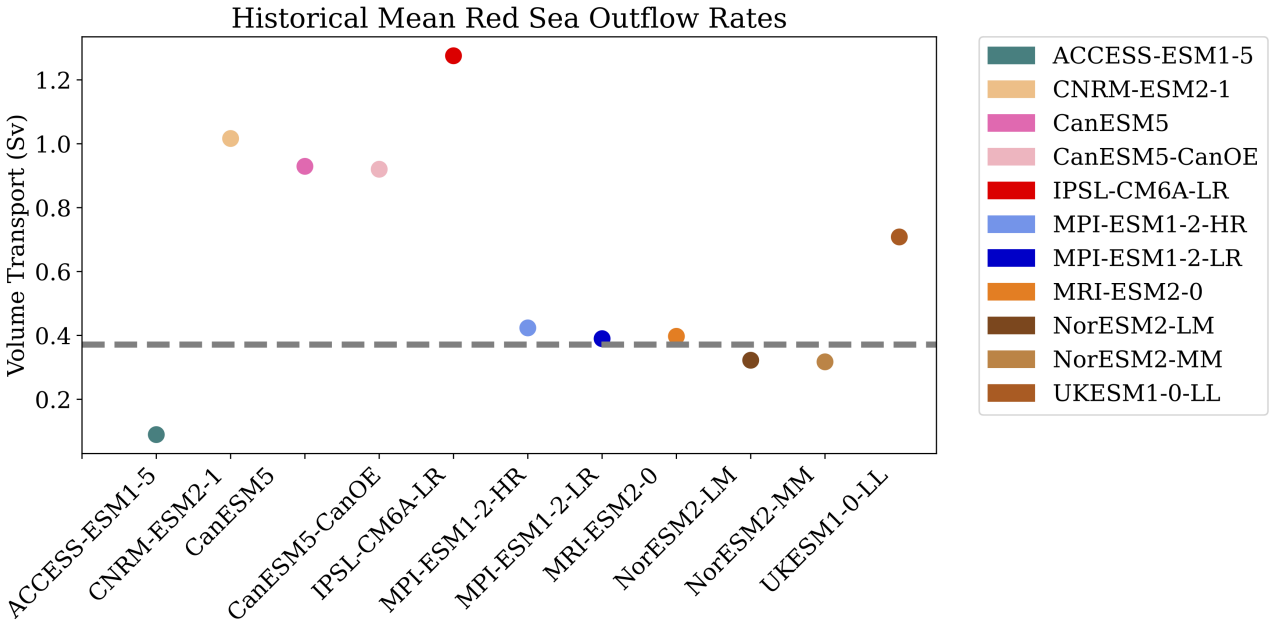

Figure S2. Mean volume transport out of the Red Sea over the historical period 1950-2015. Dashed gray line represents annual average observed outflow rate from Sofianos and Johns (2007). Red box around discarded ESMs. Transport fields for GFDL-CM4, GFDL-ESM4 and MIROC-ES2L unavailable.

Swart, N. C., Cole, J. N., Kharin, V. V., Lazare, M., Scinocca, J. F., Gillett, N. P., Anstey, J., Arora, V., Christian, J. R., Jiao, Y., Lee, W. G., Majaess, F., Saenko, O. A., Seiler, C., Seinen, C., Shao, A., Solheim, L., von Salzen, K., Yang, D., Winter, B., and Sigmond, M.: CCCma CanESM5 model output prepared for CMIP6 CMIP, https://doi.org/10.22033/ESGF/CMIP6.1303, 2019a.

Swart, N. C., Cole, J. N., Kharin, V. V., Lazare, M., Scinocca, J. F., Gillett, N. P., Anstey, J., Arora, V., Christian, J. R., Jiao, Y., Lee, W. G., Majaess, F., Saenko, O. A., Seiler, C., Seinen, C., Shao, A., Solheim, L., von Salzen, K., Yang, D., Winter, B., and Sigmond, M.: CCCma CanESM5-CanOE model output prepared for CMIP6 CMIP, https://doi.org/10.22033/ESGF/CMIP6.10205, 2019b.

Swart, N. C., Cole, J. N., Kharin, V. V., Lazare, M., Scinocca, J. F., Gillett, N. P., Anstey, J., Arora, V., Christian, J. R., Jiao, Y., Lee, W. G., Majaess, F., Saenko, O. A., Seiler, C., Seinen, C., Shao, A., Solheim, L., von Salzen, K., Yang, D., Winter, B., and Sigmond, M.: CCCma CanESM5-CanOE model output prepared for CMIP6 ScenarioMIP, https://doi.org/10.22033/ESGF/CMIP6.10207, 2019c.

Swart, N. C., Cole, J. N., Kharin, V. V., Lazare, M., Scinocca, J. F., Gillett, N. P., Anstey, J., Arora, V., Christian, J. R., Jiao, Y., Lee, W. G., Majaess, F., Saenko, O. A., Seiler, C., Seinen, C., Shao, A., Solheim, L., von Salzen, K., Yang, D., Winter, B., and Sigmond, M.: CCCma CanESM5 model output prepared for CMIP6 ScenarioMIP, https://doi.org/10.22033/ESGF/CMIP6.1317, 2019d.

Talley, L. D.: Descriptive physical oceanography: an introduction, Academic press, 2011.

Yukimoto, S., Koshiro, T., Kawai, H., Oshima, N., Yoshida, K., Urakawa, S., Tsujino, H., Deushi, M., Tanaka, T., Hosaka, M., Yoshimura, H., Shindo, E., Mizuta, R., Ishii, M., Obata, A., and Adachi, Y.: MRI MRI-ESM2.0 model output prepared for CMIP6 CMIP, https://doi.org/10.22033/ESGF/CMIP6.621, 2019a.

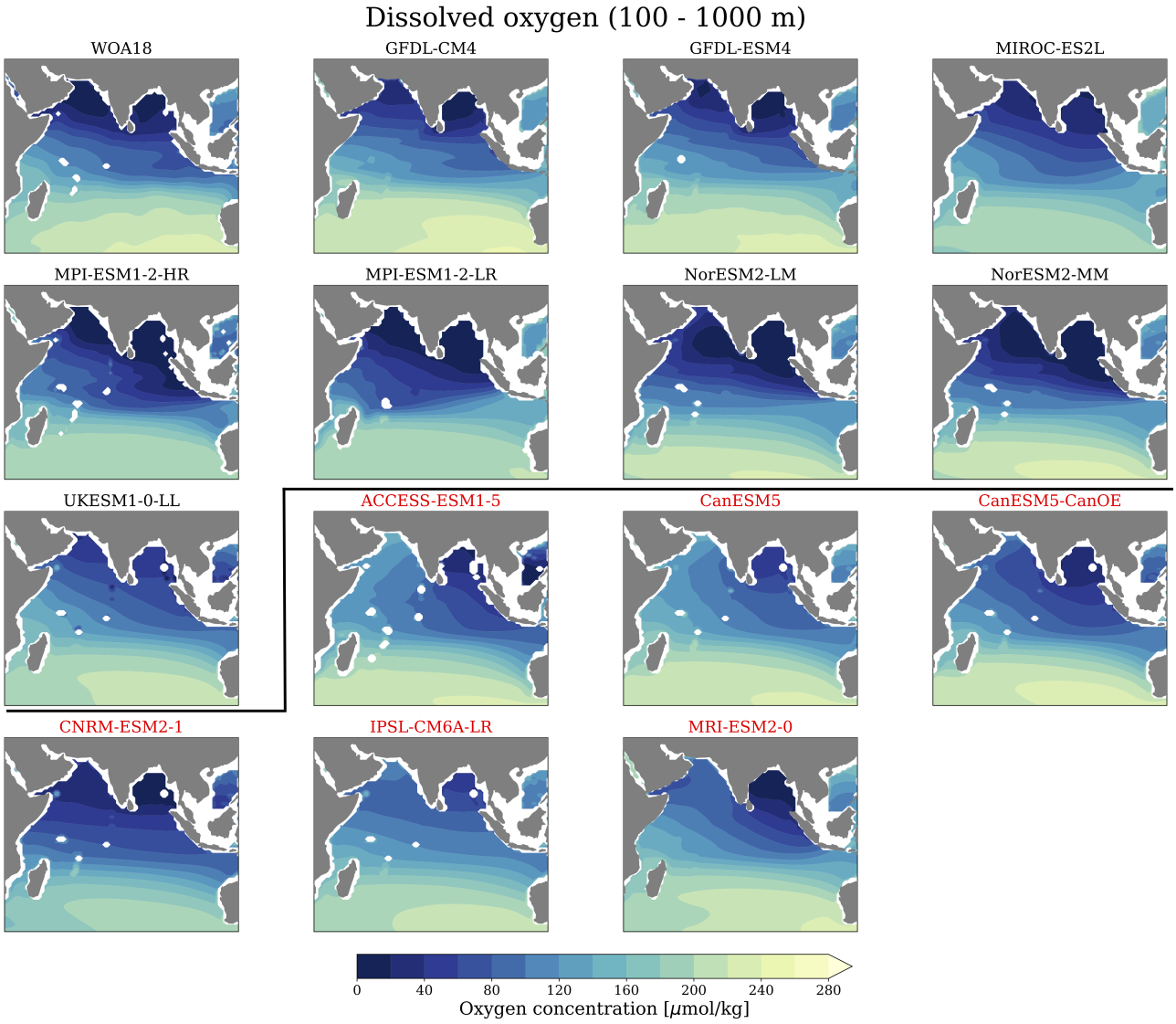

Figure S3. Maps of dissolved oxygen averaged between 100 and 1000 m in the Indian Ocean for observed climatology (WOA18) and individual CMIP6 ESMs. Models labeled in black are used in the ESM ensemble, while models labeled in red have been omitted.

Yukimoto, S., Koshiro, T., Kawai, H., Oshima, N., Yoshida, K., Urakawa, S., Tsujino, H., Deushi, M., Tanaka, T., Hosaka, M., Yoshimura, H., Shindo, E., Mizuta, R., Ishii, M., Obata, A., and Adachi, Y.: MRI MRI-ESM2.0 model output prepared for CMIP6 ScenarioMIP, https://doi.org/10.22033/ESGF/CMIP6.638, 2019b.

Ziehn, T., Chamberlain, M., Lenton, A., Law, R., Bodman, R., Dix, M., Wang, Y., Dobrohotoff, P., Srbinovsky, J., Stevens, L., Vohralik, P., Mackallah, C., Sullivan, A., O'Farrell, S., and Druken, K.: CSIRO ACCESS-ESM1.5 model output prepared for CMIP6 CMIP, https://doi.org/10.22033/ESGF/CMIP6.2288, 2019a.

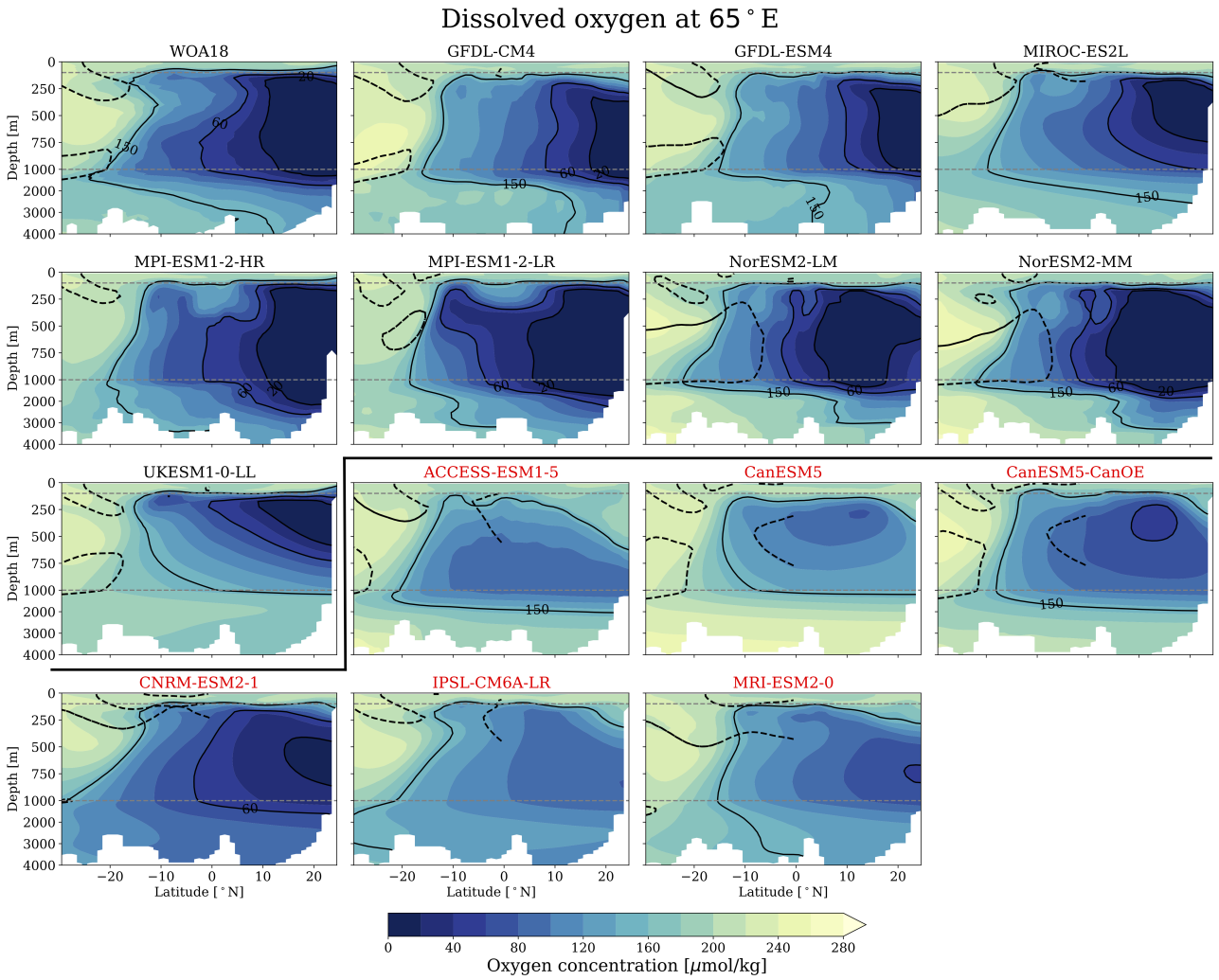

Figure S4. Sections of dissolved oxygen along 65° E in the Indian Ocean for observed climatology (WOA18) and individual CMIP6 ESMs. Contours show 20, 60, and 150 μmol/kg oxygen extent. Models labeled in black are used in the ESM ensemble, while models labeled in red have been omitted.

Ziehn, T., Chamberlain, M., Lenton, A., Law, R., Bodman, R., Dix, M., Wang, Y., Dobrohotoff, P., Srbinovsky, J., Stevens, L., Vohralik, P., Mackallah, C., Sullivan, A., O'Farrell, S., and Druken, K.: CSIRO ACCESS-ESM1.5 model output prepared for CMIP6 ScenarioMIP, https://doi.org/10.22033/ESGF/CMIP6.2291, 2019b.

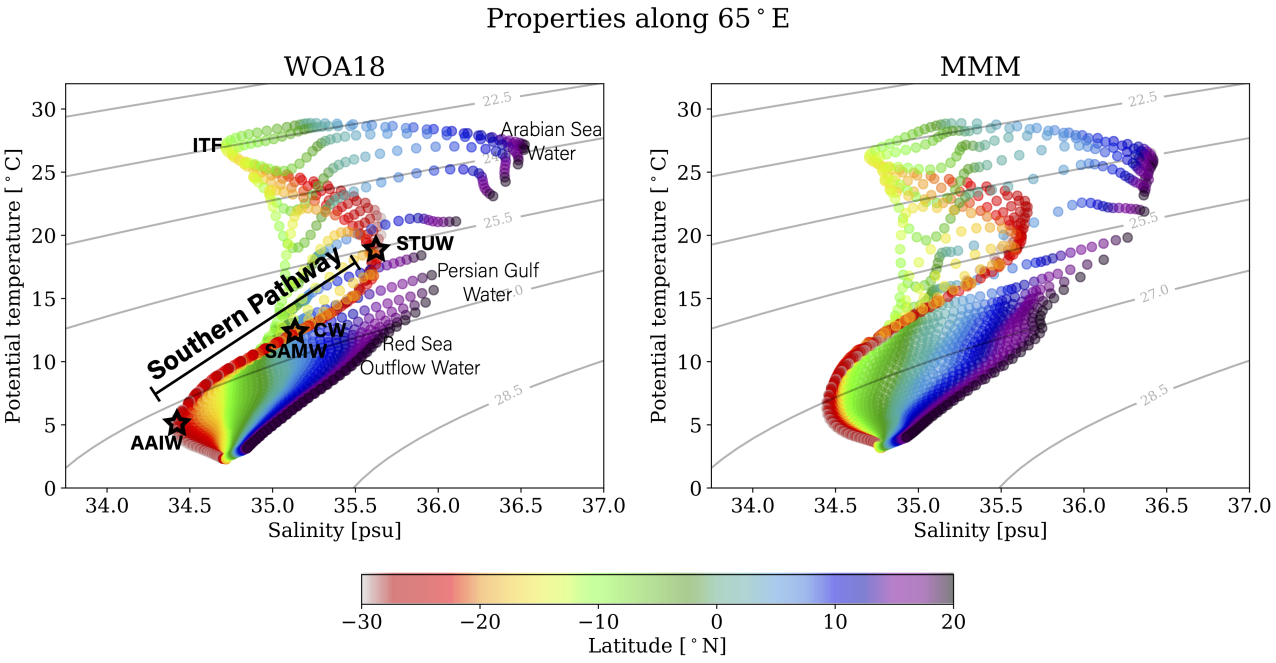

Figure S5. Temperature-Salinity relationship along 65°E between 30°S-20°N from 0-2000 m in World Ocean Atlas 2018 (WOA18) and 8-ESM multi-model mean (MMM). Water Mass Abreviations: Antarctic Intermediate Water (AAIW), Subantarctic Mode Water (SAMW), Central Water (CW), Subtropical Underwater (STUW), Indonesian Throughflow water (ITF). Potential density contours are referenced to surface pressure (σ_0). Similar to 11.18b from Talley (2011).

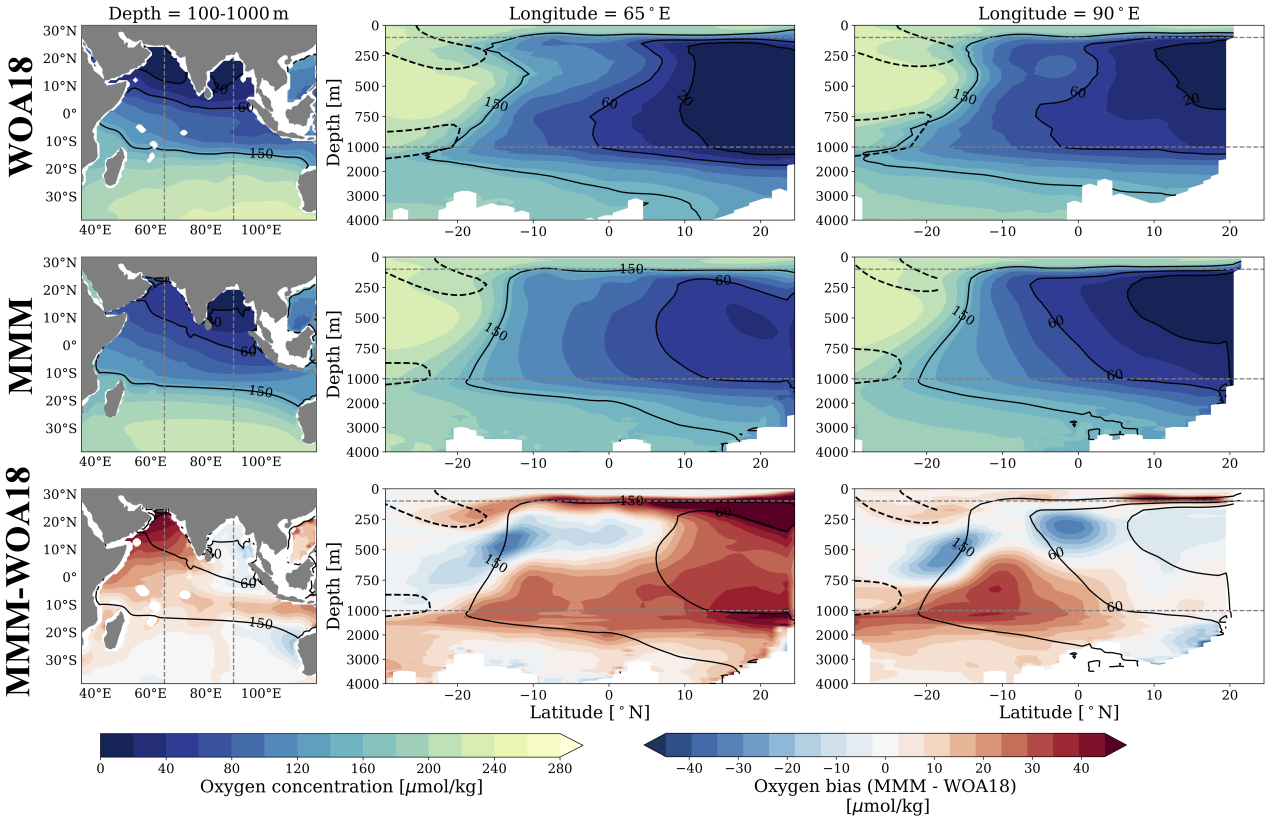

Figure S6. Same as figure 2, for all 14 CMIP6 ESMs with oxygen output. **(a-c)** Multi-Model Mean (MMM) dissolved oxygen in the Indian Ocean for historical period (1950-2015) **(a)** between 100 and 1000 m, **(b)** at 65°E, and **(c)** at 90°E. **(d-f)** Difference between MMM (1950-2015) and observed (WOA18) dissolved oxygen in the Indian Ocean **(d)** between 100 and 1000 m, **(e)** at 65°E, and **f)** at 90°E. **(a-f)** Thin solid black contours represent 150 μmol/kg in MMM, thick solid black contours represent 60 μmol/kg. Dashed contours in **(b,c,e,f)** represent salinity signatures of Subtropical Underwater (STUW) and Intermediate Water (IW), with Central Water (CW) and Mode Water (MW) between the contours (water masses labeled in panel **(b)**). Dashed gray lines represent **(a,d)** represent 65°E and 90°E and **(b,c,d,f)** 100 and 1000 m.

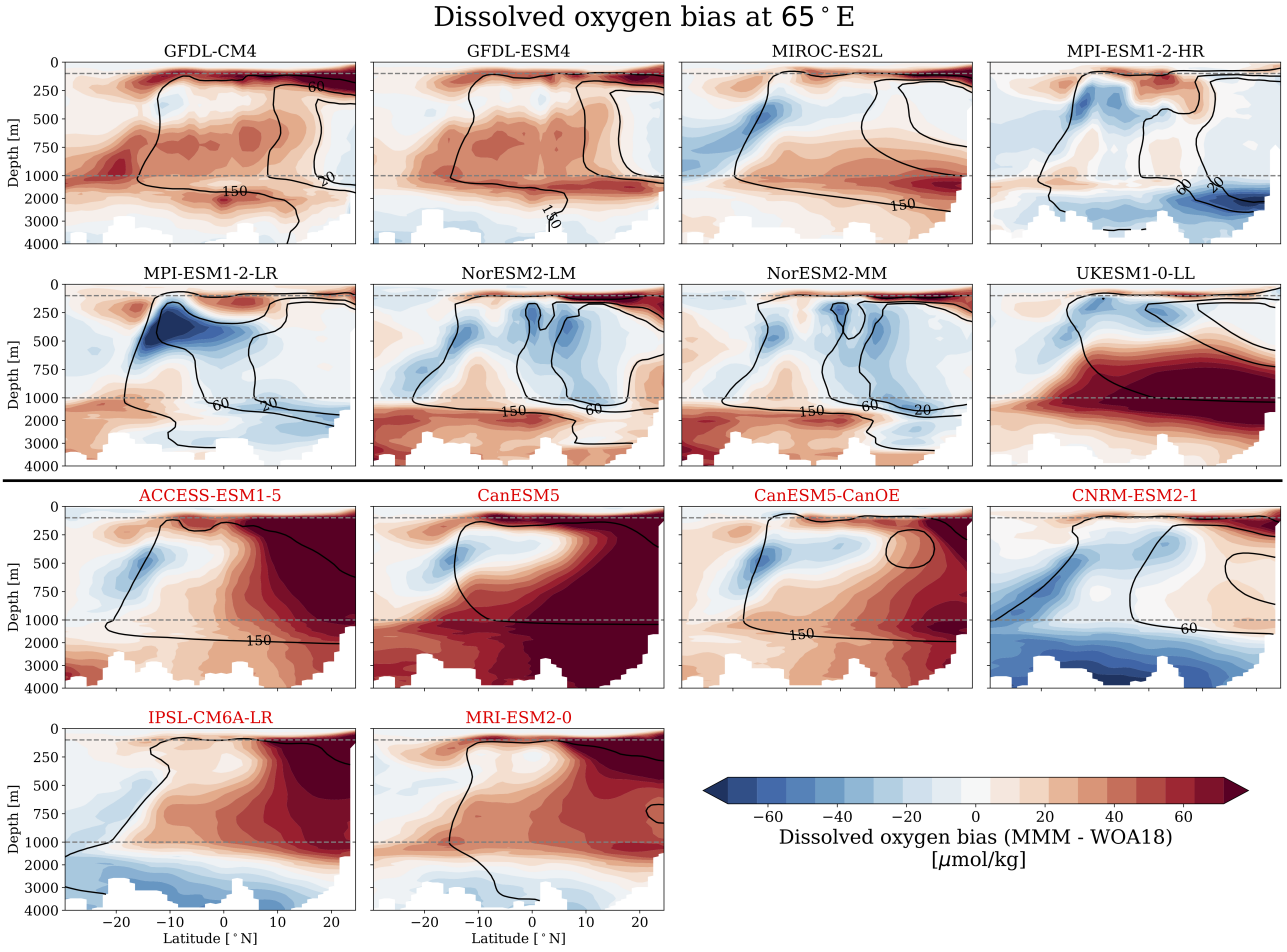

Figure S7. Sections of dissolved oxygen bias with respect to observed climatology (WOA18) along 65° E in the Indian Ocean for individual CMIP6 ESMs. Contours show 20, 60, and 150 μmol/kg oxygen extent. Models labeled in black are used in the ESM ensemble, while models labeled in red have been omitted.

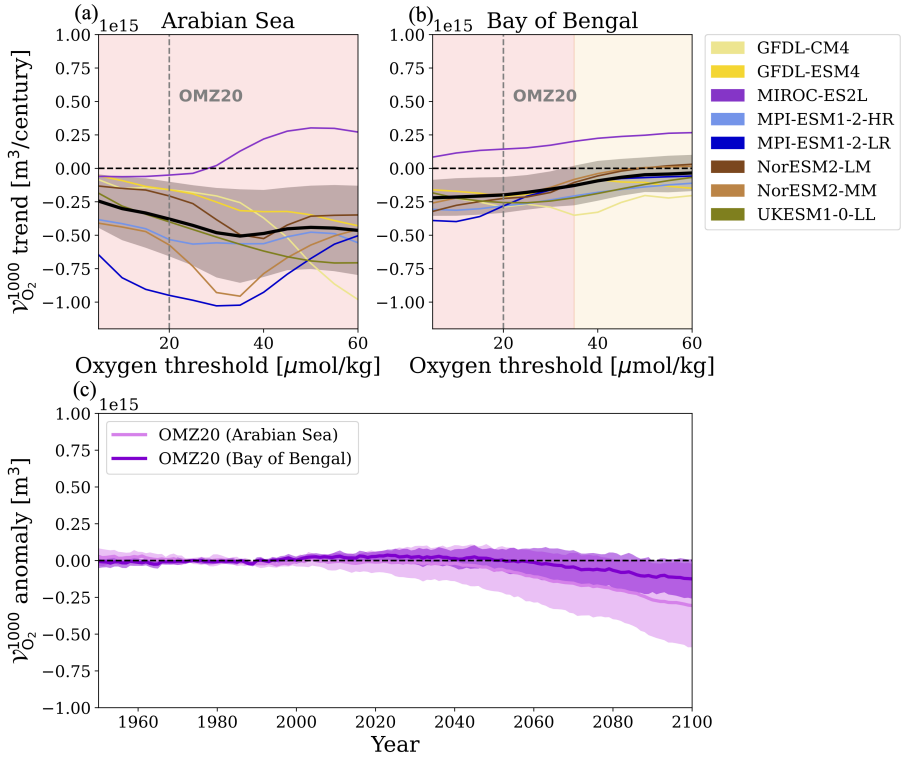

Figure S8. Multi-model mean thermocline OMZ volume changes (between 0 - 1000 m) under SSP5-8.5 scenario forcing (2015-2100) for the **(a)** Arabian Sea and **(b)** Bay of Bengal. The 20, 60 and 150 μmol/kg thresholds bounding OMZ 20, OMZ60 and OMZ150 are indicated with gray dashed lines. **(b)** Time series of $\mathcal{V}_{O_2^{1000}}$ anomaly from 1950-2100 (anomaly referenced to 1950-2015 mean) for OMZ20 in the Arabian Sea and Bay of Bengal. Shading represents one standard deviation of model spread.

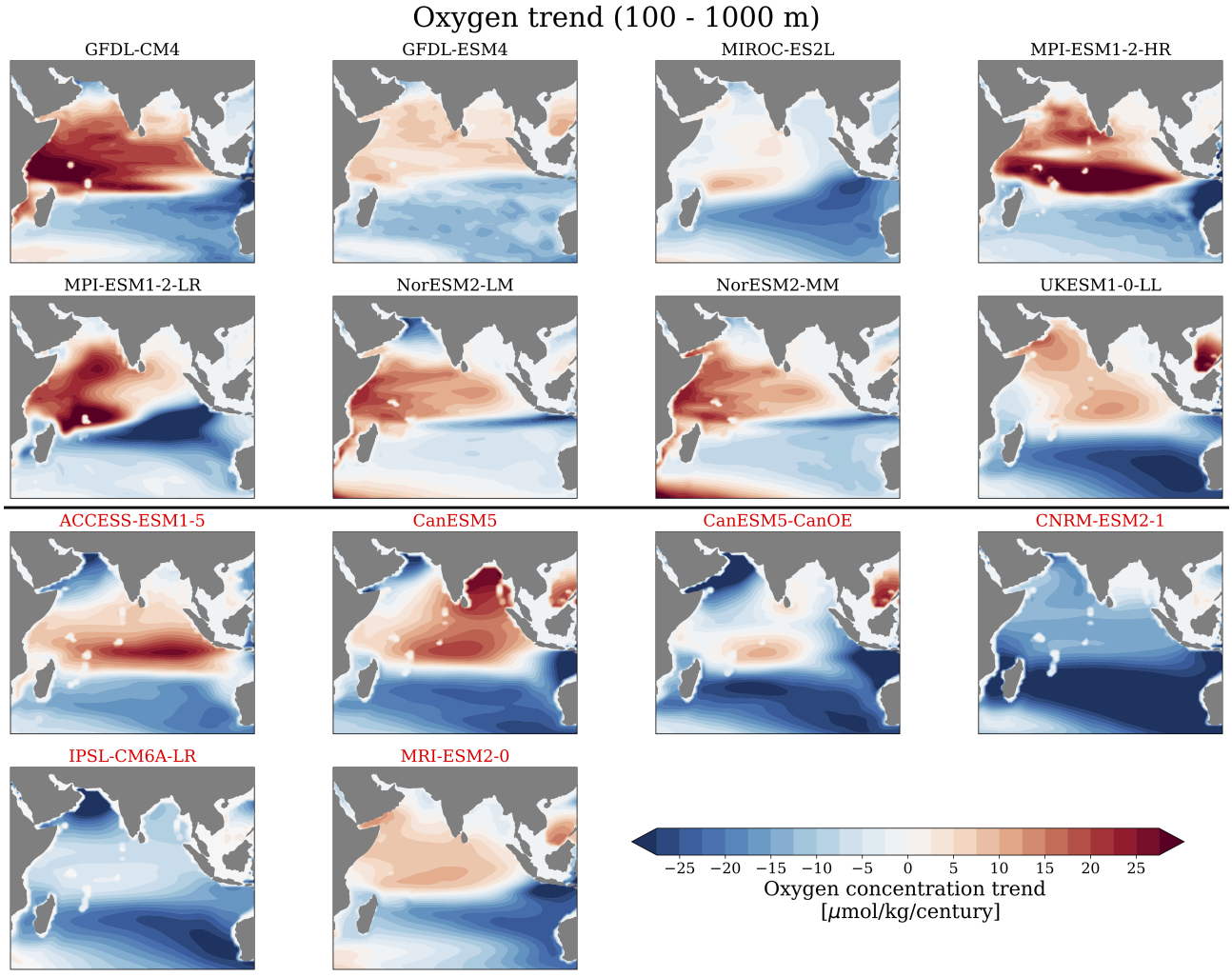

Figure S9. Maps of dissolved oxygen trends in the Indian Ocean averaged between 100 and 1000 m for individual CMIP6 ESMs. Models labeled in black are used in the ESM ensemble, while models labeled in red have been omitted (see methods).

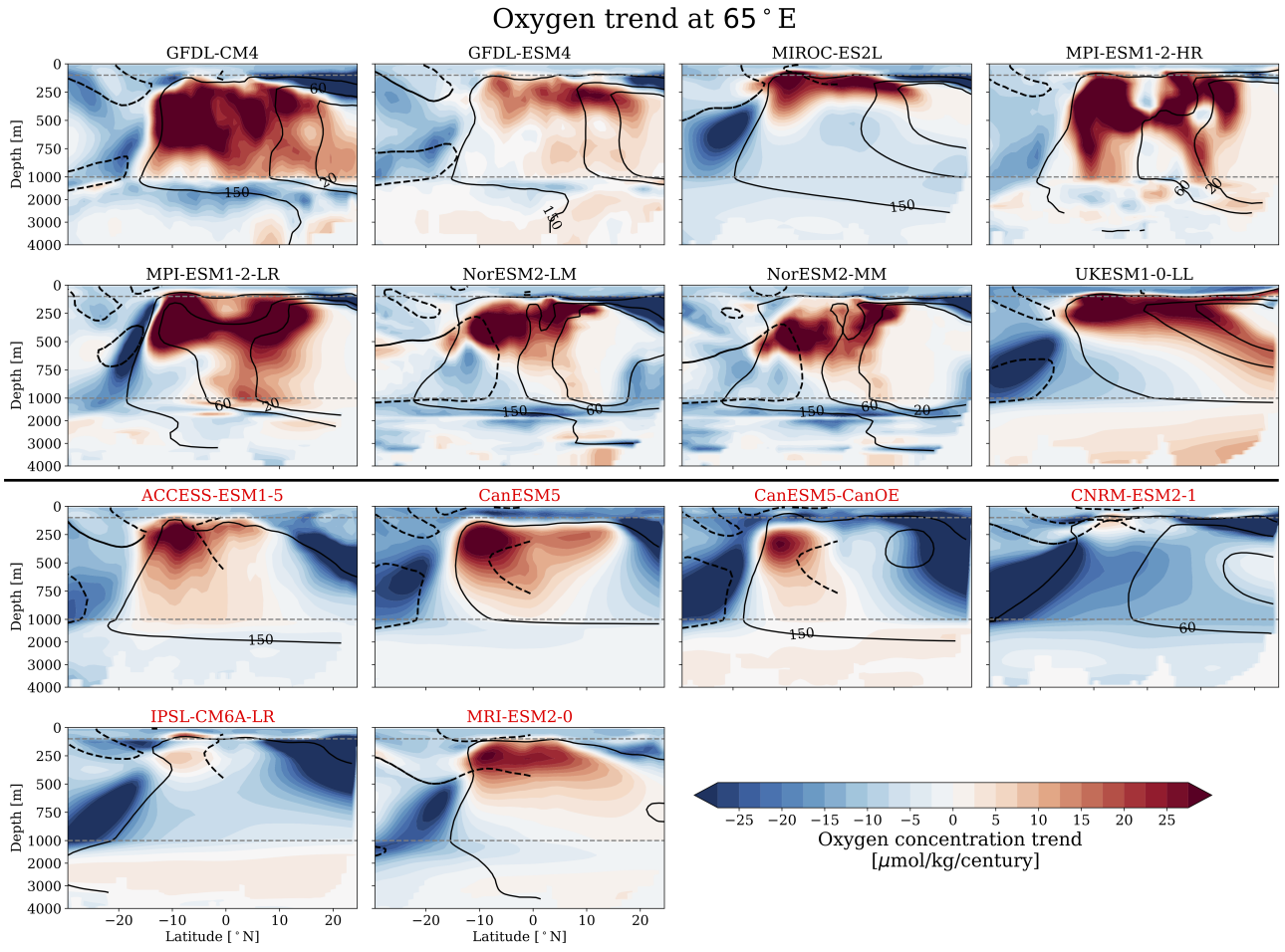

Figure S10. Sections of dissolved oxygen trends along 65° E in the Indian Ocean individual CMIP6 ESMs. Contours show 20, 60, and 150 μmol/kg oxygen extent. Models labeled in black are used in the ESM ensemble, while models labeled in red have been omitted (see methods).

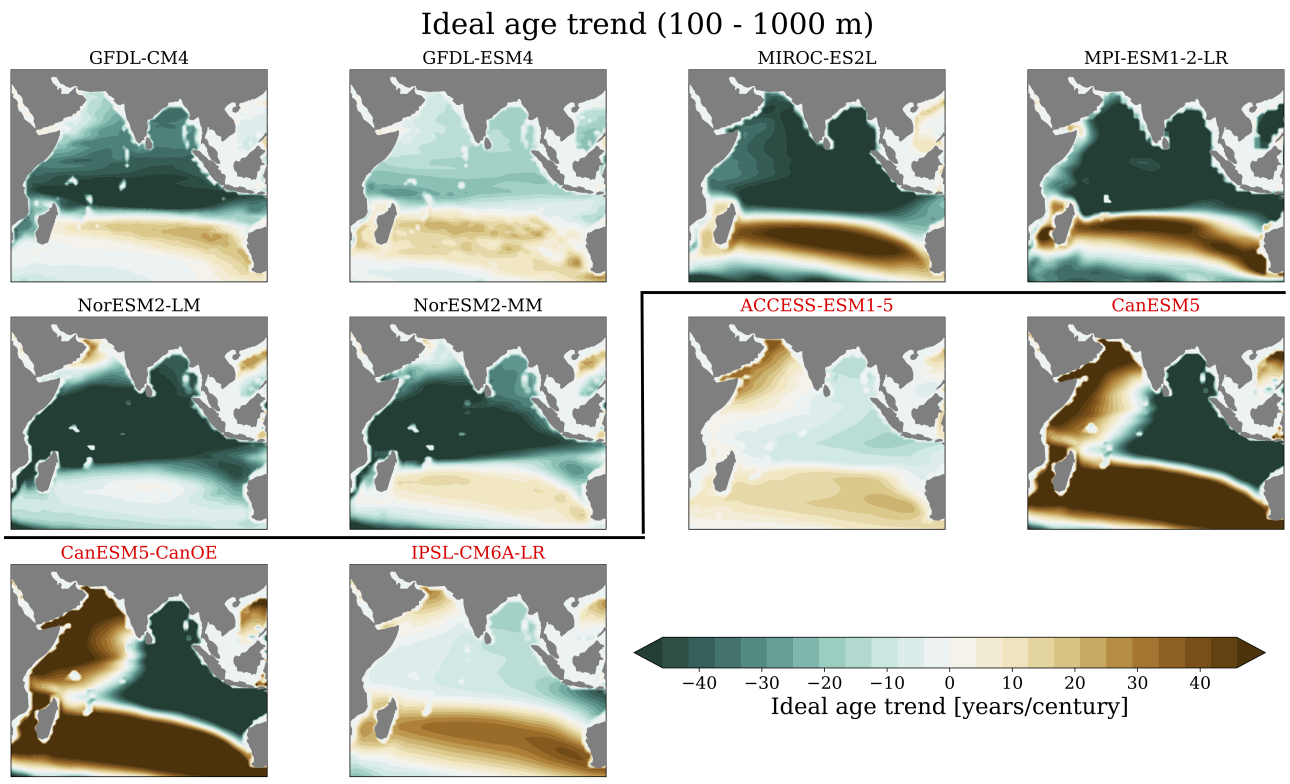

Figure S11. Maps of ideal age trends averaged between 100 and 1000 m in the Indian Ocean individual CMIP6 ESMs. Models labeled in black are used in the ESM ensemble, while models labeled in red have been omitted.

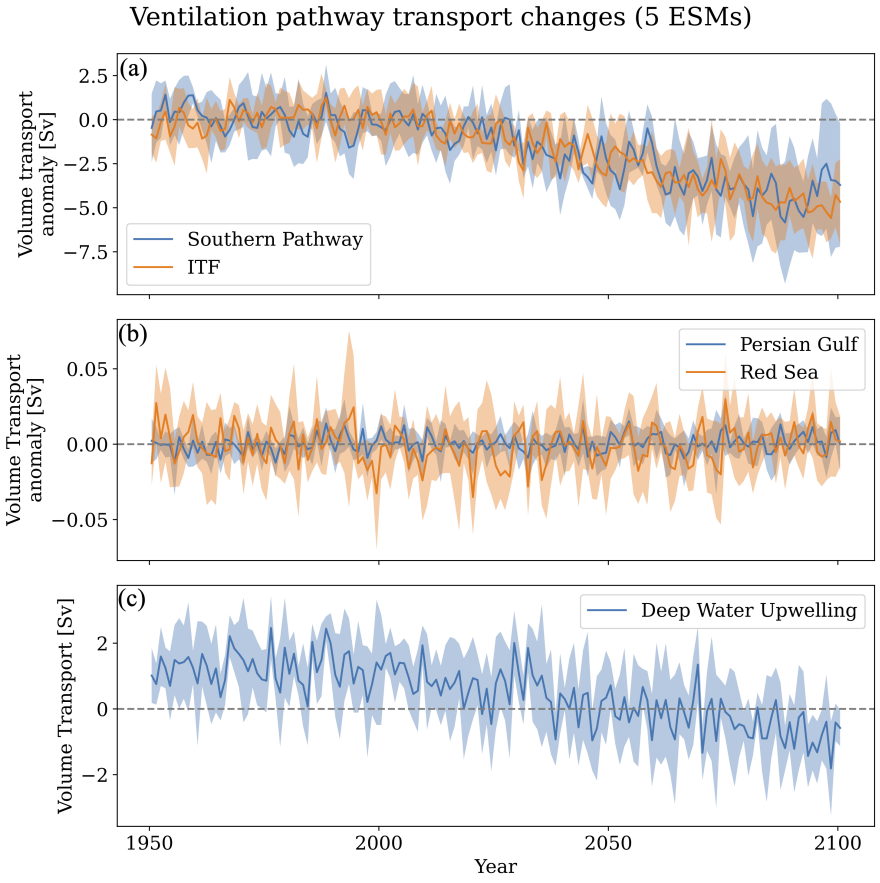

Figure S12. Volume transport anomaly timeseries for **(a)** inflowing components of Indonesian Throughflow Water and Southern Pathway Water between 100 and 1000 m and **(b)** outflowing components of Persian Gulf and Red Sea outflows. Anomalies calculated with respect to 1950-2015 mean. **(c)** Volume transport timeseries for Deep Waters upwelling across 1000 m in the Indian Ocean.

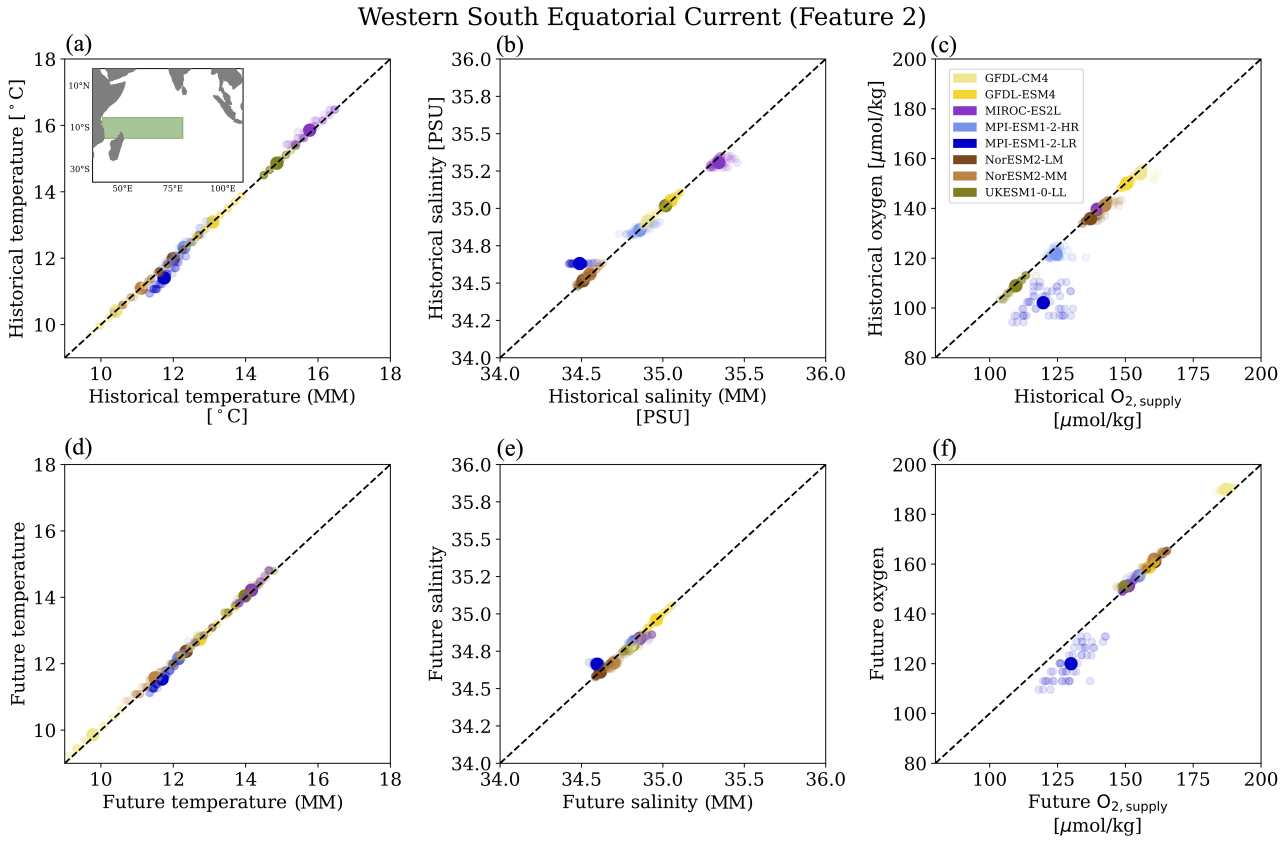

Figure S13. Evaluation of mixture model (MM) analysis in the western South Equatorial Current for historical (1950-2015) **(a)** potential temperature, **(b)** salinity, and **(c)** dissolved oxygen, and future (climatological 2100) **(d)** potential temperature, **(e)** salinity, and **(f)** dissolved oxygen. For dissolved oxygen, remineralization can cause points to fall below the 1-to-1 line.

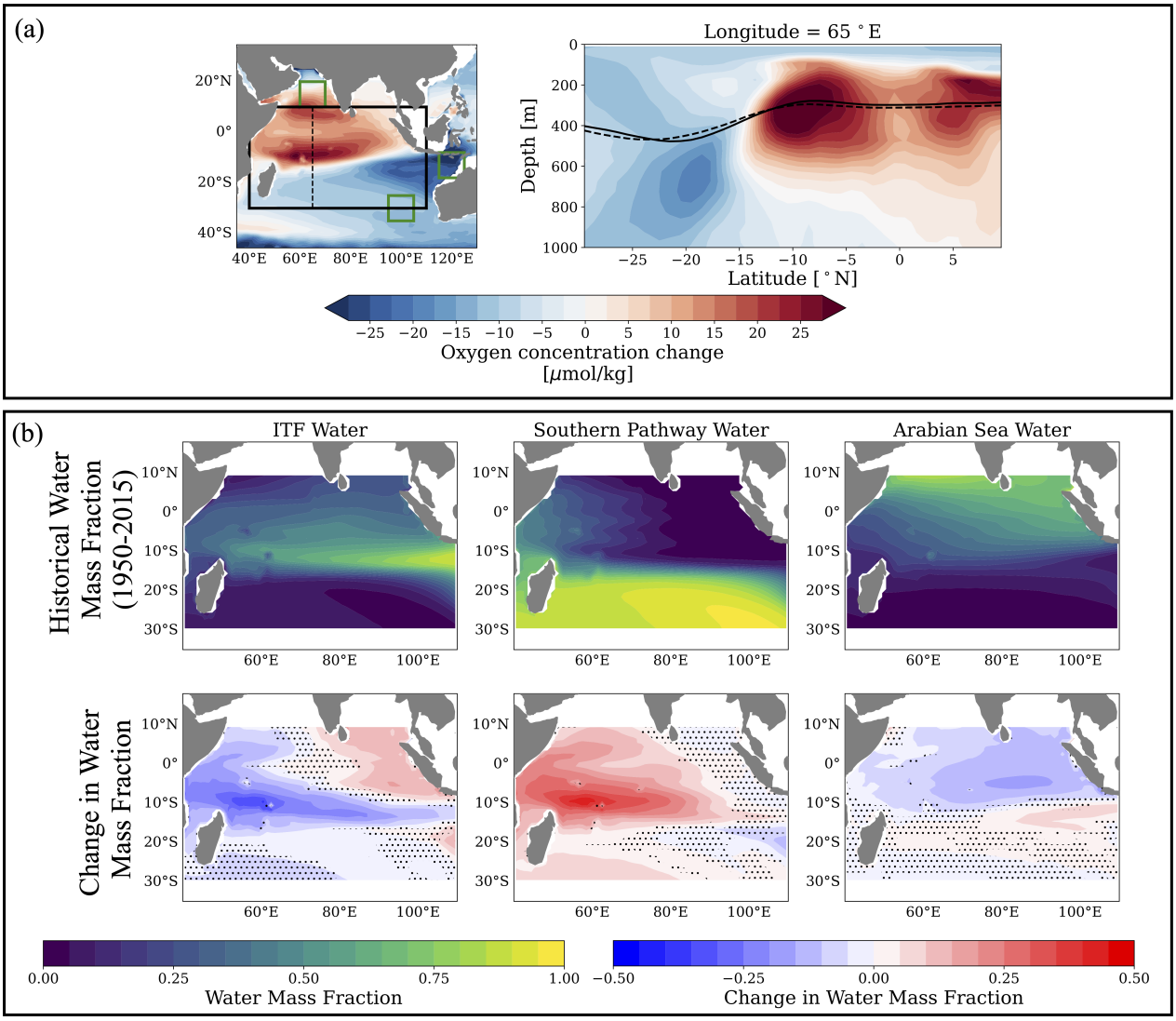

Figure S14. Alternative mixture model for the South Equatorial Current comparing historical and future density layers which occupy similar depths

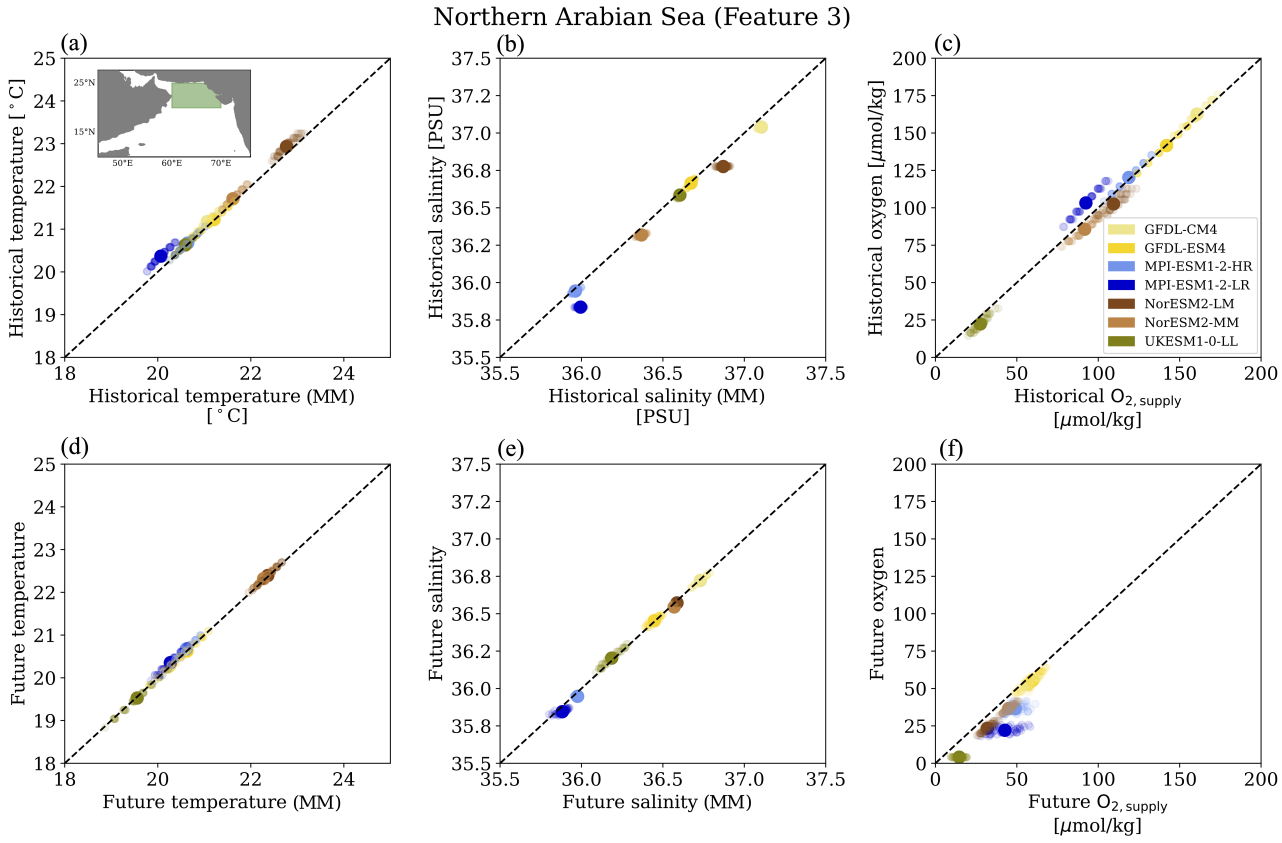

Figure S15. Evaluation of mixture model (MM) analysis in the northern Arabian Sea for historical (1950-2015) **(a)** potential temperature, **(b)** salinity, and **(c)** dissolved oxygen, and future (climatological 2100) **(d)** potential temperature, **(e)** salinity, and **(f)** dissolved oxygen. For dissolved oxygen, remineralization can cause points to fall below the 1-to-1 line.

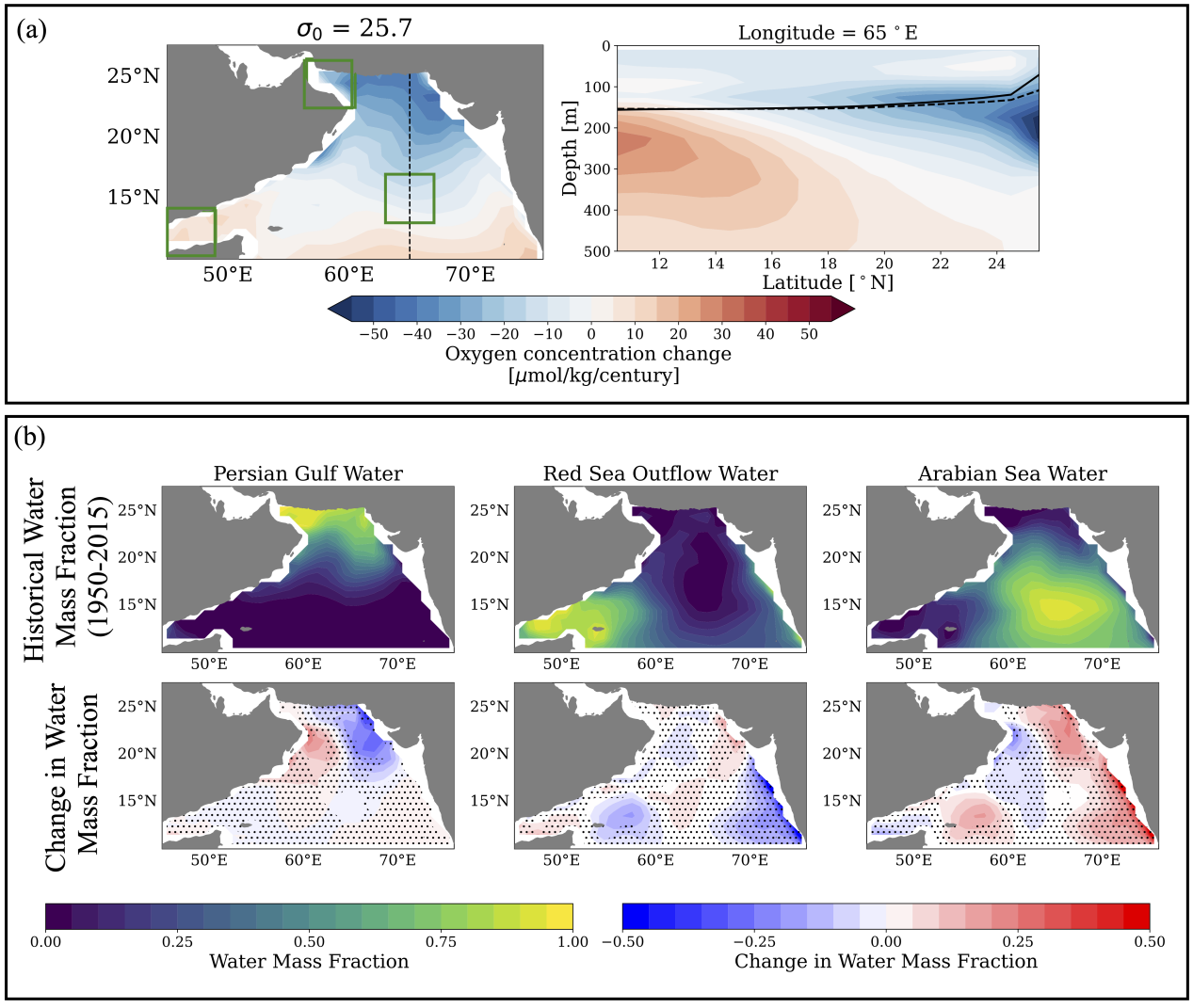

Figure S16. Alternative mixture model for Arabian Sea comparing historical and future density layers which occupy similar depths

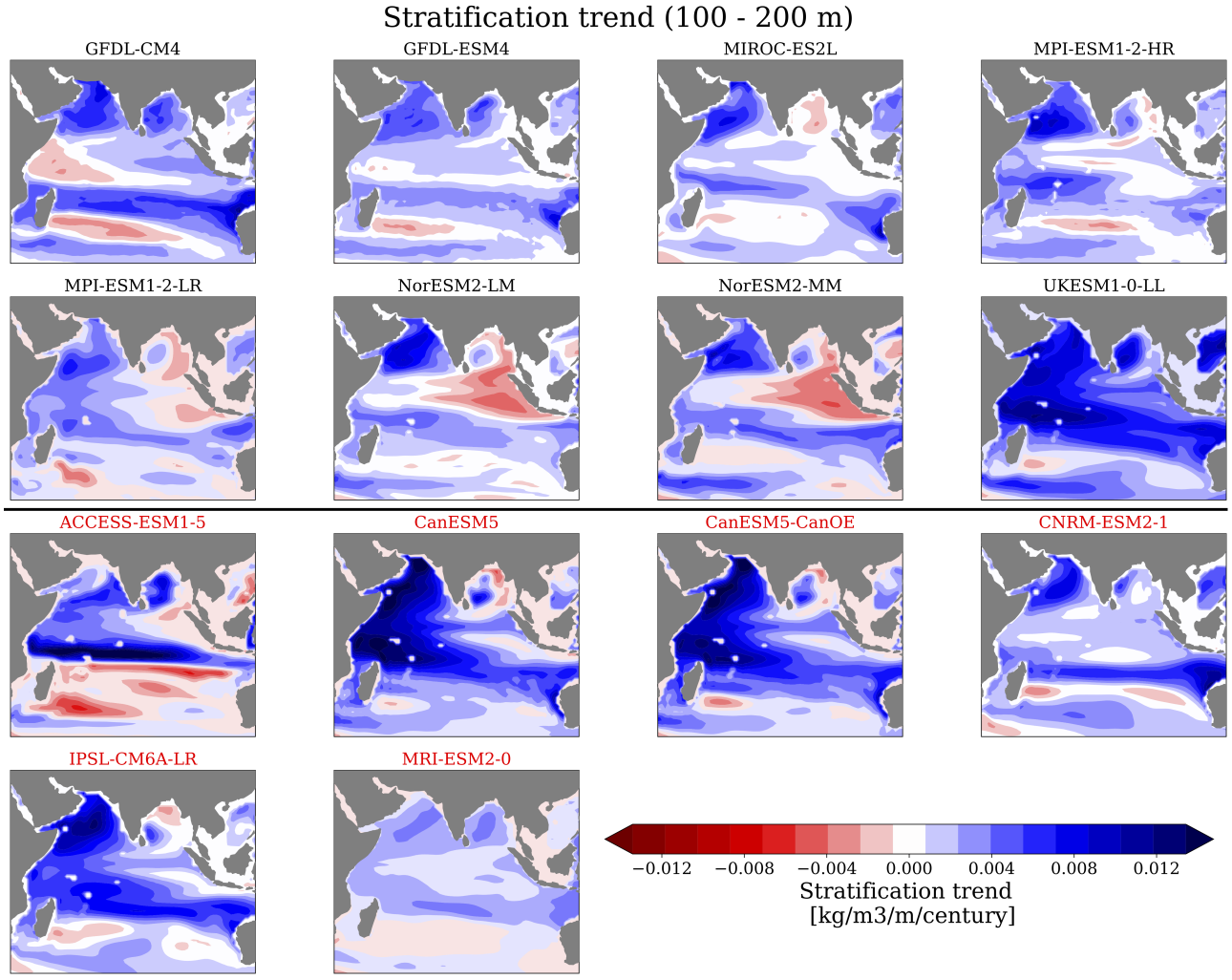

Figure S17. Maps of stratification trends averaged between 100 and 200 m in the Indian Ocean for individual CMIP6 ESMs. Models labeled in black are used in the ESM ensemble, while models labeled in red have been omitted.

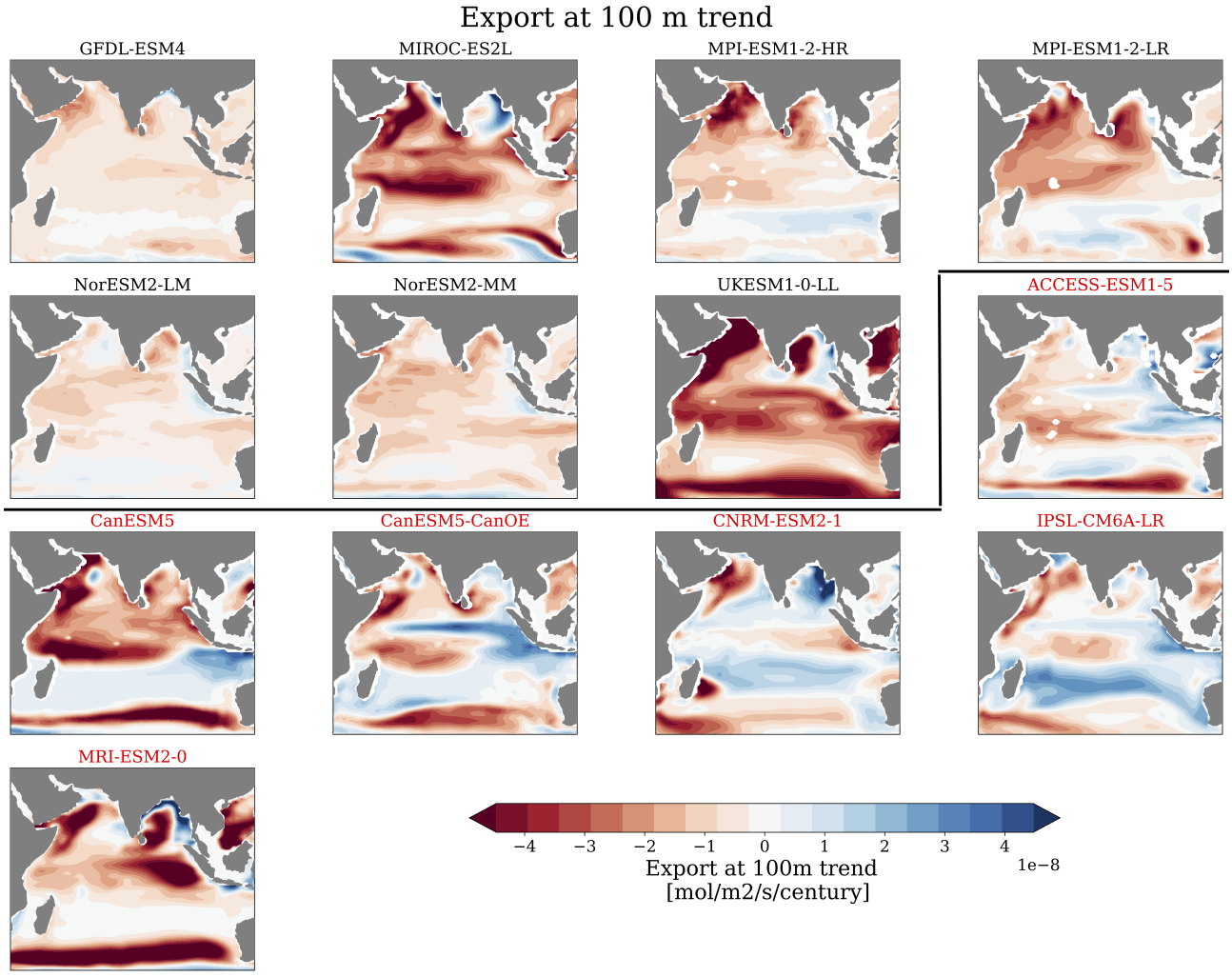

Figure S18. Maps of trends in export of carbon at 100 m in the Indian Ocean for individual CMIP6 ESMs. Models labeled in black are used in the ESM ensemble, while models labeled in red have been omitted.

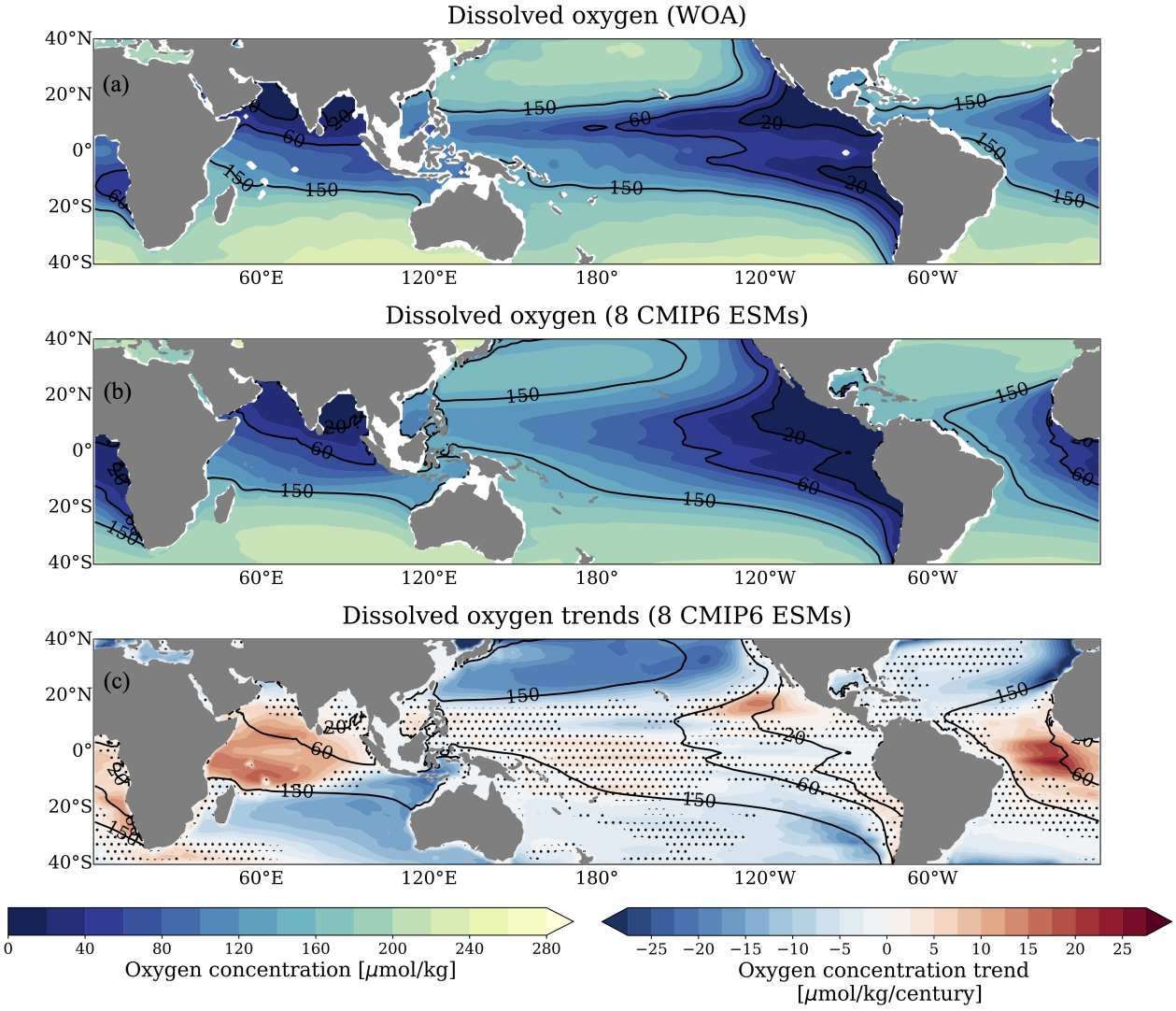

Figure S19. Maps of dissolved oxygen in the global tropical ocean averaged between 100 and 1000 m for **(a)** World Ocean Atlas and **(b)** Multi model mean of 8 CMIP6 ESMs. **(c)** Multi-model mean dissolved oxygen trends under SSP5-8.5 scenario forcing (2015-2100) between 100 and 1000 m. Solid black contours represent 20, 60 and 150 μmol/kg oxygen. Results are stippled where less than 75% (6/8) of models agree on sign of trend.